Investigating the Pressure-Induced Amorphization of Zeolitic Imidazolate Framework ZIF-8: Mechanical Instability Due to Shear Mode Softening

Aurélie U. Ortiz,[†] Anne Boutin,[‡] Alain H. Fuchs,[†] and François-Xavier Coudert*,[†]

[†]CNRS and Chimie ParisTech, 11 rue Pierre et Marie Curie, 75005 Paris, France

[‡]Département de Chimie, École Normale Supérieure, CNRS-ENS-UPMC, 24 rue Lhomond, 75005 Paris, France

S *Supporting Information*

ABSTRACT: We provide the first molecular dynamics study of the mechanical instability that is the cause of pressure-induced amorphization of zeolitic imidazolate framework ZIF-8. By measuring the elastic constants of ZIF-8 up to the amorphization pressure, we show that the crystal-to-amorphous transition is triggered by the mechanical instability of ZIF-8 under compression, due to shear mode softening of the material. No similar softening was observed under temperature increase, explaining the absence of temperature-induced amorphization in ZIF-8. We also demonstrate the large impact of the presence of adsorbate in the pores on the mechanical stability and compressibility of the framework, increasing its shear stability. This first molecular dynamics study of ZIF mechanical properties under variations of pressure, temperature, and pore filling opens the way to a more comprehensive understanding of their mechanical stability, structural transitions, and amorphization.

SECTION: Surfaces, Interfaces, Porous Materials, and Catalysis
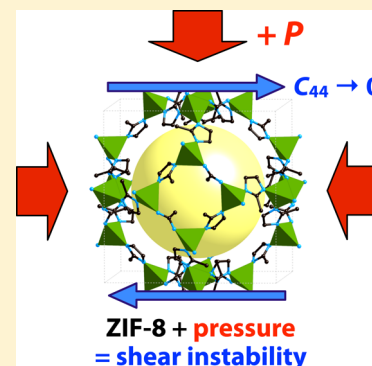
Z eolitic imidazolate frameworks (ZIFs) are a subclass of metal−organic frameworks (MOFs)[1−4] that feature imidazolate linkers bridging metal centers to form 3D porous crystalline solids isomorphous to zeolitic frameworks.[5−8] ZIFs have recently gained considerable attention for their potential applications because they inherit desirable qualities from both worlds: the tunable porosity, structural flexibility, and the functionalization of the internal surface of the MOFs as well as the thermal, mechanical, and chemical stability of the zeolites. Moreover, the similarities between the metal−imidazolate four-fold coordination chemistry and the corner-sharing SiO_4 tetrahedra from which zeolites are built mean that many ZIF topologies can potentially be synthesized. Indeed, over 100 different ZIF structures have been reported so far. Theoretical[9,10] as well as experimental[11] investigations of the relative stabilities of these structures indicate that they have a relatively low enthalpy of formation, and that many more polymorphs should be accessible under mild synthesis conditions. The ZIF structures reported in the literature so far demonstrate a large gamut of attractive structural and physicochemical properties, with great potential for applications in fluid separation,[12−15] CO_2 capture,[16] sensing,[17] and encapsulation and controlled delivery.[18]

Given their larger number of potential applications, issues of thermal and mechanical stability of flexible MOFs in general[19−21] and ZIFs in particular[22] are of high importance. A number of recent studies have addressed the question of ZIF stability at high temperature, showing temperature-induced amorphization of some ZIFs (ZIF-1, ZIF-3, ZIF-4),[23] while others do not amorphize at high temperature (including the prototypical ZIF-8).[24] All ZIF frameworks studied so far have shown pressure-induced amorphization at modest, industrially accessible pressure. ZIF-8[5] (Figure 1) undergoes irreversible
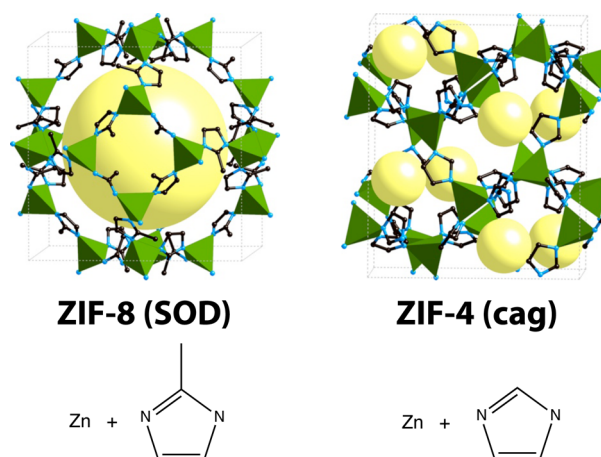

Figure 1. Imidazolate linker, structure, and network topology of ZIF-4 and ZIF-8. Yellow spheres represent the free volume within the frameworks.

amorphization under nonhydrostatic mechanical compression as low as 0.3 GPa[25] as well as under ball-milling.[26] The pressure-induced amorphization of ZIF-4[5] (Figure 1) was also studied: Bennett et al.[27] showed that amorphization occurs at various values of hydrostatic pressure depending on the presence or absence of solvent molecules in the pores of the material, as well as the nature of the hydrostatic medium. The evacuated ZIF-4 demonstrated amorphization at very low pressure (0.35 GPa), while the presence of DMF molecules in its pores could shift amorphization to higher pressure and lead to the existence of an intermediate monoclinic crystalline phase (ZIF-4-I).

While all of the experimental studies of pressure-induced amorphization cited above have taken great care in identifying the structure of the various amorphous ZIF phases, there is a lack of experimental information on the nature of the crystal-to-amorphous transition, the reasons behind its occurrence, and its apparent universality under mechanical pressure. This is in good part because the amorphization happens at such low pressure that little data is available on the stressed ZIFs. Furthermore, a recent study by Tan et al.[22] measured the shear modulus of ZIF-8, which they find to be quite low, at ~1 GPa. Tan et al. also suggested that the pressure-induced amorphization of ZIF-8 may be linked to this low shear modulus. However, the pressure-induced amorphization is observed at pressure lower than 1 GPa, and in addition, a direct link between these two properties has yet to be demonstrated. In this work, we report the evolution of the mechanical properties of ZIF-8 as a function of both external stress and adsorbate loading to elucidate the nature of the pressure-induced crystal-to-amorphous transition.

Figure 2 presents the evolution of the unit cell parameter and elastic constants of ZIF-8 as a function of mechanical pressure,
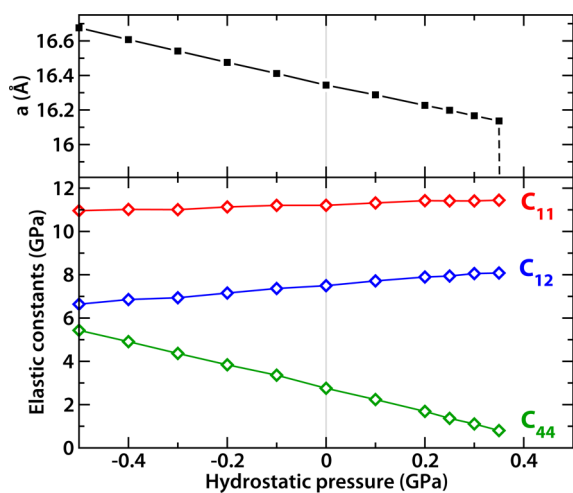

Figure 2. Unit cell parameter a and elastic constants C_{11}, C_{12}, and C_{44} of ZIF-8 as a function of hydrostatic pressure at 77 K.

at 300 K, for an isotropic compression corresponding to hydrostatic experimental conditions with a nonpenetrating hydrostatic fluid. Both the average lattice parameters and the elastic constants were obtained from constant-stress (N, σ, T) molecular dynamics (MD) simulations by analysis of the fluctuations of unit cell vectors[28,29] (the so-called strain-fluctuation method), where the elastic stiffness tensor C_{ijkl} is obtained by:

$$\left(\frac{k_B T}{V}\right) C_{ijkl}^{-1} = \langle \varepsilon_{ij} \varepsilon_{kl} \rangle - \langle \varepsilon_{ij} \rangle \langle \varepsilon_{kl} \rangle \tag{1}$$

where ε is the unit cell strain and V is the unit cell volume. We described the fully flexibly ZIF-8 framework using the force field of Zhang et al, which was calibrated to reproduce the ZIF-8 structure, bulk modulus, and sorption-induced structural transformation.[30] (See the Supporting Information for simulation details.)

First, direct observation of the MD trajectories shows that the ZIF-8 framework is stable at pressures lower than 0.4 GPa but unstable at higher pressure. In the range of pressures from −0.5 to 0.35 GPa (where negative pressure indicates tension and positive pressure indicates compression), ZIF-8 shows linear elasticity with a bulk modulus of $E = 8$ GPa, in good agreement with the values determined experimentally (from Brillouin scattering: 7.7 GPa;[21] from pressure-induced lattice variations: 6.5 GPa[24]). At $P \geq 0.4$ GPa, however, we observe a rapid collapse of the framework, demonstrating its instability under pressure. The value of this critical pressure is, again, in good agreement with the experimental data of Chapman et al., who observed amorphization beyond 0.34 GPa under hydrostatic conditions.[25]

To find the fundamental cause of this instability we look at the evolution of the elastic constants of ZIF-8 as a function of applied pressure (Figure 2, bottom panel). Because the ZIF-8 framework is cubic, its mechanical properties are fully described by only three elastic constants: C_{11}, C_{12}, and C_{44}, which are, respectively, the modulus for axial compression, dilation on compression, and shear. First, we see that the values obtained for the unstressed crystal ($P = 0$) using this methodology are in good agreement with the experimental values obtained by Brillouin scattering: the agreement is very good for C_{11} and C_{12} (this work: 11.3 and 7.6 GPa; ref 22: 9.5 and 6.9 GPa) and reasonable for C_{44} (2.7 GPa vs 0.97 GPa) considering how challenging the accurate prediction of absolute values of elastic constants is. More important is the pressure-dependence of the elastic constants, where we can see that C_{44} diminishes drastically under compression of the crystal, a phenomenon known as *shear-mode softening*. This decrease leads to elastic instability of the ZIF-8 framework because the Born stability conditions for a cubic crystal under hydrostatic pressure P can be written as:[31]

$$C_{11} + 2C_{12} + P \geq 0; \quad C_{11} - C_{12} \geq 2P; \quad C_{44} \geq P \tag{2}$$

At $P = 0.4$ GPa, the third condition, which indicates stability under shear deformation, breaks down and the ZIF-8 framework becomes mechanical unstable. We thus conclude that the amorphization of ZIF-8 under pressure is triggered by elastic instability, itself due to a pressure-induced softening of the (already relatively soft) shear deformation mode of the material. While it is the first time such a mechanism is demonstrated for amorphization of a MOF, it is known to be the underlying cause of pressure-induced phase transitions in some dense inorganic solids (e.g., the halite-CsCl-type transition of MgO or the stishovite-CaCl$_2$-type transition in SiO$_2$[32]) as well as the pressure-induced amorphization of coesite.[33]

In their recent study of ZIF-4 amorphization, Bennett et al.[27] have demonstrated that both the onset of amorphization and the bulk modulus of ZIF-4 depend highly on the presence or absence of solvent molecules in their pores. In particular, they showed that the evacuated framework was much more flexible.

Moreover, it was shown in some soft porous crystals, such as the MIL-53 family, that adsorption-induced stress can lead to structural transitions of large amplitude.[34] These considerations are of critical importance for practical applications in real conditions. We have thus investigated the elastic constants and mechanical stability of ZIF-8 with methane adsorbed inside its pores. Methane was chosen as a generic guest molecule for this study because of its apolar nature and the absence of specific guest−ZIF interactions to better understand the generic effect of pore volume filling on mechanical properties. Table 1 reports

Table 1. Elastic Constants of the ZIF-8 Framework at 300 K for Various Values of CH_4 Loading at 300 K and 0 GPa

CH_4/unit cell	C_{11} (GPa)	C_{12} (GPa)	C_{44} (GPa)
0	11.21	7.49	2.75
3	11.26	7.52	2.89
6	11.29	7.55	2.96
11	11.33	7.58	3.18
18	11.38	7.66	4.00

the evolution of ZIF-8 elastic constants for CH_4 loadings between 0 and 18 molecules per unit cell (which corresponds to methane uptake at 100 bar and 300 K; see the isotherm in Figure S1 in the Supporting Information). Whereas the effect of pore filling is modest on the C_{11} and C_{12} elastic constants, it drastically increases the shear modulus of ZIF-8, with a variation of C_{44} from 2.7 GPa in the evacuated material to 4.0 GPa with 18 methane molecules per unit cell. This increased resistance to shear is directly linked to the higher density of the guest-filled material, for which a shear motion implies a larger number of repulsive guest−guest and guest−host close contacts, as shown by Coasne et al. in zeolites.[35]

Moreover, MD simulations of ZIF-8 at this loading and under hydrostatic compression have revealed its increased mechanical stability compared to the empty ZIF-8: the material is stable under compression up to 0.65 GPa, while it collapses at higher pressure. The pressure dependence of the elastic constants is shown in Figure 3 in the form of the stability criteria for compression ($\lambda = C_{11} - C_{12} - 2P$) and shear ($\mu = C_{44} - P$), both of which must be positive for the system to be
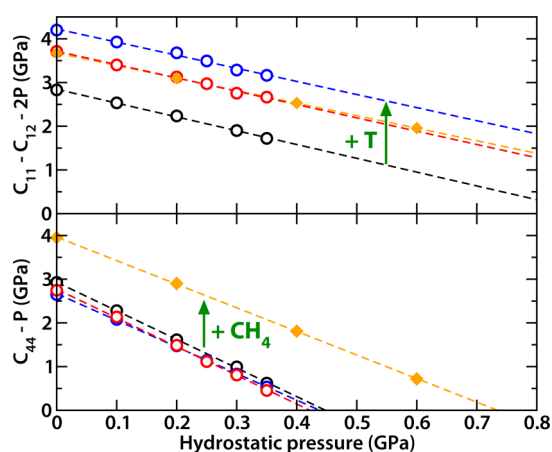

Figure 3. Evolution of the stability criteria for compression (upper panel, $\lambda = C_{11} - C_{12} - 2P$) and shear (lower panel, $\mu = C_{44} - P$) of ZIF-8 as a function of hydrostatic pressure. Black: empty ZIF-8 at 77 K; red: empty ZIF-8 at 300 K; blue: empty ZIF-8 at 500 K; orange: ZIF-8 with 18 CH_4 at 300 K.

mechanically stable. Figure 3 demonstrates that pressure-induced amorphization in methane-loaded ZIF-8 is, like the evacuated material, triggered by a mechanical instability due to shear softening but that the onset of amorphization is delayed due to the larger shear modulus of the unstressed material. We also plot on Figure 3 the evolution of elastic constants at 77 and 500 K. No temperature-induced softening is observed: C_{44} is almost unchanged, while C_{11} actually increases. The absence of elastic softening at higher temperature is in good agreement with the fact that no amorphization of ZIF-8 upon heating has been reported in the literature.

Preliminary results on the elastic constants and mechanical stability of the ZIF-4 framework under hydrostatic pressure (Figure S2 in the Supporting Information) point to the same mechanism for its pressure-induced amorphization. A softening of the shear modes (three of them because the ZIF-4 framework is orthorhombic) is also found to be associated with mechanical instability under compression, although the value of transition pressure obtained by this study does not fall in line with the experimental results, and further work needs to be done to refine the force field used for the simulation to account for the differences in coordination bonds and angles between ZIF-8 (for which the force field was optimized) and ZIF-4. Nonetheless, the fact that the very different ZIF-8 and ZIF-4 frameworks both undergo pressure-induced amorphization due to shear instability hints that the phenomenon may be generic. We thus conclude that the crystalline porous ZIF phases, although they retain zeolite-like framework topologies, do not possess the mechanical stability of zeolites because of the weaker Zn−imidazolate coordinative bonds compared with the strong Si−O bond. Moreover, their very high porosity gives rise to low resistance to shear and pressure-induced shear softening, which in turn is the cause for their mechanical instability at low pressure.

Finally, it should be noted that whereas the molecular dynamics simulations reported in this work are helpful to understand how the mechanical instability of ZIFs develops depending on thermodynamic conditions, they unfortunately cannot yield direct information on the nature of the amorphous phase obtained and do not explain why the amorphous phase is preferred to a hypothetical denser crystalline phase. All simulations of ZIF-8 at high pressure, in which the framework collapses, lead to the occurrence of a denser porous crystalline phase of $Zn(mim)_2$, with reduced pore volume compared with ZIF-8. This can be attributed to the limitations of the force field used: by its bonded nature, it does not allow reconstructive transitions to take place in the system. DFT-based molecular dynamics simulations would allow a direct simulation of the amorphization process, but the computational cost of such simulations on a large-scale supercell of ZIF-8 is not within our reach.

In conclusion, we have determined that the mechanism of pressure-induced amorphization of ZIF-8 is a pressure-induced mechanical instability due to shear mode softening. The shear modulus (C_{44}) of the ZIF-8 cubic framework, which was shown by previous work to be quite low, actually decreases under compression of the framework. We find that temperature changes do not induce instability of the framework, consistent with the absence of temperature-induced amorphization of ZIF-8. We show that the presence of guest molecules in the highly porous ZIF-8 greatly increases its resistance to shear, requiring a higher pressure to amorphize. In essence, we highlight how constant-stress molecular dynamics can be used to investigate

1863

dx.doi.org/10.1021/jz400880p | J. Phys. Chem. Lett. 2013, 4, 1861−1865

pressure- and temperature-induced amorphization and structural transitions.

■ ASSOCIATED CONTENT

Ⓢ Supporting Information

Molecular simulation details, values of elastic constants, and methane adsorption isotherms. This material is available free of charge via the Internet at http://pubs.acs.org.

■ AUTHOR INFORMATION

Corresponding Author

*E-mail: fx.coudert@chimie-paristech.fr.

Notes

The authors declare no competing financial interest.

■ ACKNOWLEDGMENTS

■ REFERENCES

(1) Horike, S.; Shimomura, S.; Kitagawa, S. Soft Porous Crystals. *Nat. Chem.* **2009**, *1*, 695−704.

(2) Farha, O. K.; Hupp, J. T. Rational Design, Synthesis, Purification and Activation of Metal-Organic Framework Materials. *Acc. Chem. Res.* **2010**, *43*, 1166−1175.

(3) Férey, G. Hybrid Porous Solids: Past, Present, Future. *Chem. Soc. Rev.* **2008**, *37*, 191−214.

(4) Tranchemontagne, D. J.; Mendoza-Cortes, J. L.; O'Keeffe, M.; Yaghi, O. M. Secondary Building Units, Nets and Bonding in the Chemistry of Metal-Organic Frameworks. *Chem. Soc. Rev.* **2009**, *38*, 1257−1283.

(5) Park, K. S.; Ni, Z.; Côté, A. P.; Choi, J. Y.; Huang, R.; Uribe-Romo, F. J.; Chae, H. K.; O'Keeffe, M.; Yaghi, O. M. Exceptional Chemical And Thermal Stability Of Zeolitic Imidazolate Frameworks. *Proc. Natl. Acad. Sci. U.S.A.* **2006**, *103*, 10186.

(6) Zhang, J.-P.; Zhu, A.-X.; Lin, R.-B.; Qi, X.-L.; Chen, X.-M. Pore Surface Tailored SOD-Type Metal-Organic Zeolites. *Adv. Mater.* **2011**, *23*, 1268−1271.

(7) Phan, A.; Doonan, C. J.; Uribe-Romo, F. J.; Knobler, C. B.; O'Keeffe, M.; Yaghi, O. M. Synthesis, Structure, And Carbon Dioxide Capture Properties Of Zeolitic Imidazolate Frameworks. *Acc. Chem. Res.* **2010**, *43*, 58−67.

(8) Zhang, J.-P.; Zhang, Y.-B.; Lin, J.-B.; Chen, X.-M. Metal Azolate Frameworks: From Crystal Engineering To Functional Materials. *Chem. Rev.* **2011**, *112*, 1001−1033.

(9) Lewis, D. W.; Ruiz-Salvador, A. R.; Gomez, A.; Rodriguez-Albelo, L. M.; Coudert, F.-X.; Slater, B.; Cheetham, A. K.; Mellot-Draznieks, C. Zeolitic Imidazole Frameworks: Structural And Energetics Trends Compared With Their Zeolite Analogues. *CrystEngComm* **2009**, *11*, 2272−2276.

(10) Baburin, I. A.; Leoni, S.; Seifert, G. Enumeration Of Not-Yet-Synthesized Zeolitic Zinc Imidazolate MOF Networks: A Topological and DFT Approach. *J. Phys. Chem. B* **2008**, *112*, 9437−9443.

(11) Hughes, J. T.; Bennett, T. D.; Cheetham, A. K.; Navrotsky, A. Thermochemistry of Zeolitic Imidazolate Frameworks of Varying Porosity. *J. Am. Chem. Soc.* **2013**, *135*, 598−601.

(12) Li, K.; Olson, D. H.; Seidel, J.; Emge, T. J.; Gong, H.; Zeng, H.; Li, J. Zeolitic Imidazolate Frameworks For Kinetic Separation Of Propane And Propene. *J. Am. Chem. Soc.* **2009**, *131*, 10368−10369.

(13) Gücüyener, C.; van den Bergh, J.; Gascon, J.; Kapteijn, F. Ethane/Ethene Separation Turned on Its Head: Selective Ethane Adsorption on the Metal-Organic Framework ZIF-7 through a Gate-Opening Mechanism. *J. Am. Chem. Soc.* **2010**, *132*, 17704−17706.

(14) Bux, H.; Feldhoff, A.; Cravillon, J.; Wiebcke, M.; Li, Y.-S.; Caro, J. Oriented Zeolitic Imidazolate Framework-8 Membrane with Sharp H_2/C_3H_8 Molecular Sieve Separation. *Chem. Mater.* **2011**, *23*, 2262−2269.

(15) Bae, T.-H.; Lee, J. S.; Qiu, W.; Koros, W. J.; Jones, C. W.; Nair, S. A High-Performance Gas-Separation Membrane Containing Submicrometer-Sized Metal-Organic Framework Crystals. *Angew. Chem., Int. Ed.* **2010**, *49*, 9863−9866.

(16) Banerjee, R.; Phan, A.; Wang, B.; Knobler, C.; Furukawa, H.; O'Keeffe, M.; Yaghi, O. M. High-Throughput Synthesis of Zeolitic Imidazolate Frameworks and Application to CO_2 Capture. *Science* **2008**, *319*, 939−943.

(17) Lu, G.; Hupp, J. T. Metal-Organic Frameworks As Sensors: A ZIF-8 Based Fabry-Pérot Device As A Selective Sensor For Chemical Vapors and Gases. *J. Am. Chem. Soc.* **2010**, *132*, 7832−7833.

(18) Liedana, N.; Galve, A.; Rubio, C.; Tellez, C.; Coronas, J. CAF@ ZIF-8: One-Step Encapsulation Of Caffeine In MOF. *ACS Appl. Mater. Interfaces* **2012**, *4*, 5016−5021.

(19) Ortiz, A. U.; Boutin, A.; Fuchs, A. H.; Coudert, F.-X. Anisotropic Elastic Properties of Flexible Metal-Organic Frameworks: How Soft are Soft Porous Crystals? *Phys. Rev. Lett.* **2012**, *109*, 195502.

(20) Ortiz, A. U.; Boutin, A.; Fuchs, A. H.; Coudert, F.-X. Metal-Organic Frameworks With Wine-Rack Motif: What Determines Their Flexibility And Elastic Properties? *J. Chem. Phys.* **2013**, *138*, 174703.

(21) De Toni, M.; Jonchiere, R.; Pullumbi, P.; Coudert, F.-X.; Fuchs, A. H. How Can a Hydrophobic MOF be Water-Unstable? Insight into the Hydration Mechanism of IRMOFs. *ChemPhysChem* **2012**, *13*, 3497−3503.

(22) Tan, J.-C.; Civalleri, B.; Lin, C.-C.; Valenzano, L.; Galvelis, R.; Chen, P.-F.; Bennett, T. D.; Mellot-Draznieks, C.; Zicovich-Wilson, C. M.; Cheetham, A. K. Exceptionally Low Shear Modulus in a Prototypical Imidazole-Based Metal-Organic Framework. *Phys. Rev. Lett.* **2012**, *108*, 095502.

(23) Bennett, T. D.; Goodwin, A. L.; Dove, M. T.; Keen, D. A.; Tucker, M. G.; Barney, E. R.; Soper, A. K.; Bithell, E. G.; Tan, J.-C.; Cheetham, A. K. Structure and Properties of an Amorphous Metal-Organic Framework. *Phys. Rev. Lett.* **2010**, *104*, 115503.

(24) Bennett, T. D.; Keen, D. A.; Tan, J.-C.; Barney, E. R.; Goodwin, A. L.; Cheetham, A. K. Thermal Amorphization of Zeolitic Imidazolate Frameworks. *Angew. Chem., Int. Ed.* **2011**, *50*, 3067−3071.

(25) Chapman, K. W.; Halder, G. J.; Chupas, P. J. Pressure-Induced Amorphization and Porosity Modification in a Metal-Organic Framework. *J. Am. Chem. Soc.* **2009**, *131*, 17546−17547.

(26) Cao, S.; Bennett, T. D.; Keen, D. A.; Goodwin, A. L.; Cheetham, A. K. Amorphization Of The Prototypical Zeolitic Imidazolate Framework ZIF-8 By Ball-Milling. *Chem. Commun.* **2012**, *48*, 7805−7807.

(27) Bennett, T. D.; Simoncic, P.; Moggach, S. A.; Gozzo, F.; Macchi, P.; Keen, D. A.; Tan, J.-C.; Cheetham, A. K. Reversible Pressure-Induced Amorphization Of A Zeolitic Imidazolate Framework (ZIF-4). *Chem. Commun.* **2011**, *47*, 7983−7985.

(28) Ray, J. R. Fluctuations and Thermodynamic Properties of Anisotropic Solids. *J. Appl. Phys.* **1982**, *53*, 6441.

(29) Parrinello, M.; Rahman, A. Strain Fluctuations and Elastic Constants. *J. Chem. Phys.* **1982**, *76*, 2662−2666.

(30) Zhang, L.; Hu, Z.; Jiang, J. Sorption-Induced Structural Transition of Zeolitic Imidazolate Framework-8: A Hybrid Molecular Simulation Study. *J. Am. Chem. Soc.* **2013**, *135*, 3722−3728.

(31) Morris, J. W., Jr.; Krenn, C. R. The Internal Stability Of An Elastic Solid. *Philos. Mag. A* **2000**, *12*, 2827−2840.

(32) Karki, B. B.; Ackland, G. J.; Crain, J. Elastic Instabilities In Crystals From Ab Initio Stress-Strain Relations. *J. Phys.: Condens. Matter* **1997**, *9*, 8579−8589.

(33) Dean, D. W.; Wentzcovitch, R. M.; Keskar, N.; Chelikowsky, J. R. Pressure-Induced Amorphization In Crystalline Silica: Soft Phonon

Modes And Shear Instabilities In Coesite. *Phys. Rev. B* **2000**, *61*, 3303−3309.

(34) Triguero, C.; Coudert, F.-X.; Boutin, A.; Fuchs, A. H.; Neimark, A. V. Understanding Adsorption-Induced Structural Transitions in Metal-Organic Frameworks: from the Unit Cell to the Crystal. *J. Chem. Phys.* **2012**, *137*, 184702.

(35) Coasne, B.; Haines, J.; Levelut, C.; Cambon, O.; Santoro, M.; Gorelli, F.; Garbarino, G. Enhanced Mechanical Strength of Zeolites by Adsorption of Guest Molecules. *Phys. Chem. Chem. Phys.* **2011**, *13*, 20096−20099.

(36) Phillips, J. C.; Braun, R.; Wang, W.; Gumbart, J.; Tajkhorshid, E.; Villa, E.; Chipot, C.; Skeel, R. D.; Kale, L.; Schulten, K. Scalable Molecular Dynamics with NAMD. *J. Comput. Chem.* **2005**, *26*, 1781−1802.

1865

dx.doi.org/10.1021/jz400880p | *J. Phys. Chem. Lett.* 2013, 4, 1861−1865